Thermodynamic Analysis of Reflected Solar Radiation on Tilted PV Module in South India

A. D. Dhass
Department of Mechanical Engineering
Indus University
Ahmedabad 382115
India

Dhiren R. Patel
Department of Mechanical Engineering
Indus University
Ahmedabad 382115
India

A substantial volume of energy is necessary for meeting the rising energy demand as a result of the rapid growth of population, and lifestyle changes of the society. Tilted PV module improves operation and reduces the risks involved in the generation, transmission, and utilization of electrical energy and thermal energy without any degradation in climatic conditions (like conventional sources of energy). Both fixed and tilted PV module systems receive high incoming solar radiation. In this study, the analysis of output current and voltage for varying tilt angles from 0^0 to 30^0 for different southern parts of India (Chennai, Bengaluru, Thiruvananthapuram, and Hyderabad) has been performed. The reflected albedo factor is considered for different locations ranging from 0.07 to 0.75 with the current-voltage performance parameters. Variations in PV module inclination angle with variations in the total solar radiation under different ground albedo values have been observed. The current and voltage changes with tilt angle at different locations have been studied. The monthly variations and temperature effects on exergy efficiency and solar radiation were analyzed.

Keywords: *Solar radiation, Isotropic model, Tilted surface, Ground albedo, PV module performance.*

1. INTRODUCTION

Solar, wind, and other forms of energy play roles in every aspect of human life on Earth. Renewable energy, such as solar, wind, and biomass, is used to control climate change and energy demand. As an alternative energy source, solar energy is the most popular option. The tilt angle of a PV (Photovoltaic) module, ground reflection properties, and local solar radiation levels all affect the amount of solar radiation received by a PV module. The tilt angle of a PV module has a significant impact on the amount of power it generates. Optimizing the PV module's tilt angle and orientation angle is typically done at a specific latitude angle to avoid utilizing a sun tracker on the PV module.PV module photocurrent is directly related to the amount of solar radiation that is absorbed by the module. With diffuse radiation, the PV module's top and bottom surfaces vary, resulting in a currency mismatch.

PV systems can produce high output and low payback periods with the consideration of cumulative solar radiation input under albedo effects [1]. Geophysical and meteorological circumstances have considerably influenced the performance of PV systems because of the amount of solar radiation that can fall on them [2]. For calculating solar radiation availability on a tilted surface, a comparative analysis of various empirical models comprising of the isotropic and anisotropic sky has been made[3]. The empirical model consists of Liu and Jordan (LJ), Koronakis model (KO), Badescu model (BA), Hay and Davis model (HD), Reindl, et al., model (RE), and Hay and Davis, and Reindl models (HDKR) considered to be analysis of the solar radiation availability. Among these models, Hay and Davis model (HD) estimates the highest amount of solar radiation during all the months in a year, while the Badescu model (BA) provides the least values on all the isotropic and anisotropic models. The conclusion is that the Badescu model (BA) provides the least statistical error and has a good agreement with the measured data [3].

Three types of solar radiation hit the PV panel: direct beam, diffuse, and reflected. In this, the quantity of diffuse radiation on the PV panel depends on the view factor. Variations in cell position and angle of inclination have a significant impact on the PV panel view factor. These variables alter the current generation of PV panels, causing changes to the view factor, and numerical expressions help to describe these changes [4]. The field experience of 51 automated meteorological stations has been examined for measuring solar radiation using solar radiation instruments [5]. Between January 2012 and March 2013, all 51 stations' measured values were 92%of the anticipated empirical model values, delivering the best and most accurate value [5]. During clear and cloudy weather, a thin covering of snow affects performance by 13% and 40%, respectively [6].

During summer, the amount of diffuse radiation falling on the PV module surface is less than the beam radiation [7].

This effect happens due to a low cloud (Low, thick clouds primarily reflect solar radiation and cool the surface of the Earth, it has high albedos; they reflect a large portion of the sun's energy) formation in summer. A fluctuation in diffuse radiation striking on a PV module ranges from 27% to 38% of the global radiation, whereas

Received: September 2021, Accepted: November 2021
Correspondence to: Dhiren R. Patel
Department of Mechanical Engineering,
Indus University, Ahmedabad 382115, India
E-mail: dhirenpatel85@gmail.com
doi: 10.5937/fme2201158D

variations in beam radiation vary from 68% to 76% of the global radiation in winter. It shows that cloud cover has a significant impact on the amount of solar energy absorbed by a PV module [8,9]. Current mismatch on the PV module fluctuates with the fraction of diffuse radiation impacted on it dependent on the PV module's width, inclination angle, and distance from two adjacent PV modules. A new interconnection method has been devised that can lessen the current mismatch between solar cells in different places [10]. The theoretical results showed a power gain variation of 1.06% for an inclination angle of 20^o and 30% for diffuse radiation. Variations seen in power gain were 12.82% for the inclination angle of 50^o, 70% for diffuse radiation [10].

In some regions, significant changes in albedo have been seen over the years, which has more pronounced effects, particularly in winter, due to the ground surface being covered with snow and looking even brighter than the sky [11]. During the summer months, the albedo and ideal tilt angle of the PV module are low in value. A solar panel's maximum power generation is affected by seasonal variations in the module's tilt angle. Changing the tilt angle monthly in selected Malaysian locations enhanced the output field synchronously with changes in the PV module's optimum tilt angle position [12]. Using mathematical formulae based on the location of the sun, researchers have created an algorithm for determining the optimal tilt and orientation of a PV panel [13].

The angle at which a PV panel should be tilted to maximize power output relies on the characteristics of solar radiation. In most cases, the ideal tilt angle is near the latitude angle of a specific site. According to both simulated and experimental results, the optimum tilt of a PV panel is related to an empirical formulation of the latitude angle at which the panel is located [14]. At a tilt angle of around $\pm 5^0$ degrees from its latitude, the tilt angle PV system produces more power. As a result, solar radiation on the PV module increases from 0.08 kWh/m^2/d to 0.7 kWh/m^2/d at the optimal tilt angle [15]. In this study, total solar radiation is varied for different PV module inclination from 0^o to 30^o, while albedo values varied from 0.07 to 0.75 at different locations. Variations in the output parameters of current and voltage for different PV module inclination angles and ground albedo in different regions of South India have been analyzed. The effect of temperature and monthly variations on solar radiation and exergy efficiency has been studied.

A greenhouse was originally developed as an incubator with a transparent cover that can store both long-wavelength thermal radiation and short-wavelength solar radiation. As a result, it provides a suitable and flexible climatic condition to produce a high yield in terms of product quantity and quality. Monitoring the local greenhouse climate is essential to the success of agricultural endeavors [16,17].

Data on global solar radiation (GSR) is useful in a wide range of engineering studies and applications. In contrast to air temperature data, GSR is less accessible. It is possible to use artificial neural networks (ANNs) to describe nonlinear systems that require fewer inputs. A neural network based on radial basis functions has been used for the estimate. Diffuse solar radiation and direct normal radiation fractions from global solar radiation can be estimated using a four-parameter model, which includes day of the year, global solar radiation, ambient temperature, and relative humidity [18-21].

Solar radiation availability has become increasingly important, and present observational networks are unable to keep up with demand. There are three main ways in which this deficiency manifests itself: low spatial coverage; a short record; and a lack of both global radiation data and sunlight duration [22,23].

Due to economic constraints, the number of radiation data collection stations is limited. As a result, a continual mapping of solar radiation via estimation is required. For the estimations, four combinations of data sets were used: day of the year, daily maximum air temperature, daily minimum air temperature, and daily mean air temperature [24,25].

Temperature, pressure, wind speed, precipitation, and relative humidity were the most commonly observed meteorological variables. However, the assessment of daily and monthly mean worldwide solar radiation was based on two empirical formulas that connect the solar radiation to sunshine duration, humidity, maximum temperature and latitude of the monitoring station, sunset hour, and declination angles of the sun [26-28].

With the help of a user-friendly software application, the best possible solution can be exported in a matter of minutes, saving both time and money. While this type of solution safeguards private company owners from making an outrageous investment, it also encourages them to invest in renewable energy technologies [29,30].

2. THEORY AND ANALYSIS

The reflective surface is almost negligible for a black body and its ground albedo value of zero has to be attained. While the white body surface and its ground albedo are the same, the other surface reflectivity ranges between zero and one. Various common surfaces' ground albedo values are included in Table 1 [4]**.** PV module performance is calculated by taking into account the variable albedo values provided by various types of ground surfaces. Details of the solar radiation availability in the South Indian zone (Chennai, Ben–Bengaluru, Thiruvananthapuram, and Hyderabad) are indicated in Figure 1. Similarly, overall, India's solar radiation availability is indicated in Figure 2.

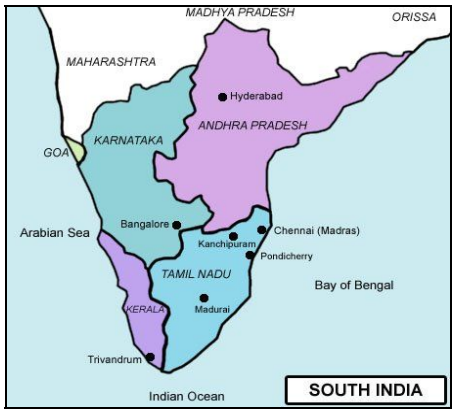

Figure1. Graphical representation of South India

Table 1. Values of reflectivity on various ground surfaces [4]

S.No	1	2	3	4	5	6	7	8	9	10	11	12	13	14	15
Surface	Snow (freshly fallen or with ice film)	Water surfaces (relatively large incidence angles)	Soils (clay, loam)	Earth roads	Coniferous forest (winter)	Forest in autumn, ripe field crops, plants	Weathered blacktop	Weathered concrete	Dead leaves	Dry grass	Green grass	Bituminous and gravel roof	Crushed rock surface	Building surfaces, dark (red brick, dark paints)	Building surfaces, light (light brick, light paints)
Average reflectivity	0.75	0.07	0.14	0.04	0.07	0.26	0.10	0.22	0.30	0.20	0.26	0.13	0.20	0.27	0.60

Table 2. Solar cell/module properties [10]

S.No	Type	Iph (A)	Is (nA)	Rs (Ω)	A	Tc (K)	Rsh (Ω)	Connection scheme
1	Cell	9.001	1.287	5.605e-3	1.091	298	1.027e3	N=1, P=1, S=1 cell
2	Module	9.001	1.287	0.336e-3	65.46	298	61.59e3	N=1, P=1, S=60 module-series

Table 3. Measured solar radiation data (from January 2014 to December 2014) [33]

Month	Monthly average total solar radiation (W/m^2)	Monthly Average daily measured sunshine duration in hours ($\overline{S}$)	Monthly average daily maximum sunshine duration in hours ($\overline{S}_0$)
January	1005	7.6752	11.3250
February	1056	9.0617	11.5941
March	1163	8.4819	11.9255
April	1178	9.3287	12.2925
May	1117	7.4430	12.6008
June	1020	6.3788	12.7530
July	942	5.4176	12.6844
August	928	5.7908	12.4222
September	960	5.6843	12.0683
October	811	5.3235	11.7016
November	751	5.4777	11.3951
December	910	6.3587	11.2483

Table 4. Mean Monthly Global and Diffuse Solar Radiant Exposure in Chennai [8]

Month	Mean monthly global solar radiant exposure		Mean monthly diffuse solar radiant exposure
	$\frac{MJ}{m^2 day}$	$\frac{W}{m^2}$	$\frac{MJ}{m^2}$
January	17.62	203.93	7.58
February	21.07	243.86	6.88
March	23.45	271.41	7.25
April	23.76	274.99	8.05
May	22.54	260.87	9.20
June	20.59	238.30	10.57
July	19.00	219.90	11.04
August	18.73	216.78	11.18
September	19.41	224.65	9.69
October	16.41	189.92	8.52
November	14.39	166.54	7.75
December	14.96	173.14	7.62

Table 5. Global and diffuse solar radiant values on cloudless days in Chennai [9]

Month	Mean monthly global solar radiant exposure on cloudless days $\frac{MJ}{m^2}$	Mean Monthly Diffuse Solar radiant Exposure on cloudless days $\frac{MJ}{m^2}$	Ratios of Diffuse to Global Solar Radiant Exposures	Ratios of Diffuse to Global Radiant Exposures on Cloudless Days
January	21.92	4.73	0.43	0.22
February	24.24	5.22	0.33	0.22
March	25.41	6.25	0.31	0.25
April	25.14	7.43	0.34	0.30
May	25.12	7.94	0.41	0.32
June	25.07	7.07	0.51	0.28
July	24.70	6.90	0.58	0.28
August	24.11	8.32	0.60	0.35
September	24.63	6.91	0.50	0.28
October	23.07	5.34	0.52	0.23
November	21.70	5.42	0.54	0.25
December	21.12	4.96	0.51	0.23

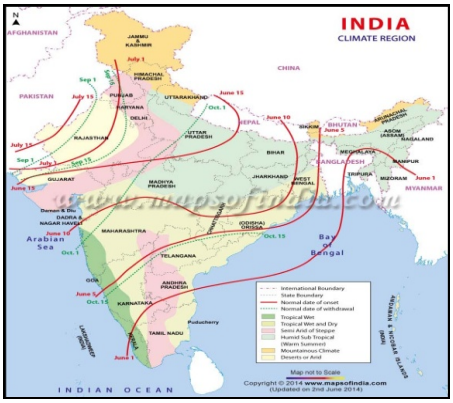

Figure 2. Availability and indication of solar radiation level in India [31]

As can be seen in Table 2, the single-cell/module has the following electrical, temperature, and connecting scheme options. It's a typical example of the work that preceded it [10]. Higher quality solar PV cells with low series resistance and high shunt have been known to exhibit short circuit current proportionate to photogenerated current in their older models [32].

2.1 Database and climate

Table 3 shows the monthly average total solar radiation, daily measured sunshine duration, and the daily maximum sunlight duration from January 2014 to December 2014 [33]. Table 4 shows the average monthly global and diffuse solar radiation measurements. The global and diffuse solar radiation, the ratio of diffuse to global solar radiant exposures, and the ratio of diffuse to global radiant exposures on cloudless days are given in Table 5. These measured values have been taken at Chennai at Latitude (N) 13^0 00', Longitude (E) $80^0$11'.

2.2 Effect of tilt and ground albedo

A simple method is to keep the best output from the PV panel at an optimum tilt angle equal to the latitude. Chennai's, latitude is 13^o and the optimum tilt angle is in the range of 10^o-15^o. Reflected solar energy and output current increased by 7.3% on the snow-covered ground, as compared with the black surface [6]. An albedo value for a given place is used to determine which tilt angle is best for that location. The location of the PV system and the albedo of the ground affect the system's optimal performance and maximum output values.

3. MODELING

3.1 Solar radiation

The monthly average of daily total radiation (H_T) on a tilted surface is the combined effect of a direct beam (H_B), diffuse beam (H_D), and reflected components of the radiation (H_R) on a tilted surface [34,35],

$$H_T = H_B + H_D + H_R \tag{1}$$

Beam radiation on a tilted surface is estimated and the conversion from solar radiation on a horizontal surface is given by,

$$H_B = \left(H_g - H_d\right) R_b \tag{2}$$

PV panel surface in the northern hemisphere sloped towards the equator is expressed as

$$R_b = \frac{\cos(\phi-)\cos(\delta)\sin(\omega'_{ss}) + \left(\frac{\Pi}{180}\right)\omega'_{ss}\sin(\phi-\beta)\sin(\delta)}{\cos(\phi)\cos(\delta)\sin(\omega_{ss}) + \left(\frac{\Pi}{180}\right)\omega_{ss}\sin(\phi)\sin(\delta)} \tag{3}$$

$$\omega_{ss} = \cos^{-1}\left(-\tan(\phi)\tan(\delta)\right),$$

$$\omega'_{ss} = \min\left\{\omega_{ss}, \cos^{-1}\left(-\tan(\phi-\beta)\tan(\delta)\right)\right\}$$

The ground-reflected radiation is given by,

$$H_R = H_g \rho\left(\frac{1-\cos\beta}{2}\right) \tag{4}$$

The diffuse radiation in the earth's atmosphere is classified into two models, namely isotropic and anisotropic models. The above model's expression is given below, For sky-diffused radiations,

$$H_D = R_d H_d \tag{5}$$

For the isotropic model (under cloudless conditions),

$$R_d = 3 + \frac{\cos(2\beta)}{2}$$

For the anisotropic model (under cloud conditions),

$$R_d = 0.51 * R_b + \left(\frac{1+\cos\beta}{2}\right) - \frac{1.74}{1.26\pi}\left[\sin\beta - \left(\frac{\beta\pi}{180}\right)\cos\beta - \pi\sin^2\left(\frac{\beta}{2}\right)\right] \quad (6)$$

The total radiation on a tilted surface is given by,

$$H_T = \left(H_g - H_d\right)R_b + H_g\rho\left(\frac{1-\cos\beta}{2}\right) + H_d R_d \quad (7)$$

The amount of photo-current generated by the PV module is directly proportional to the incident of solar radiation ($I_{ph}(H_T)$) on the surface and is expressed as,

$$I_{ph}\left(H_T\right) = I_{ph}\left(H_0\right) * \frac{H_T}{H_0} \quad (8)$$

where H_0 is an extra-terrestrial daily radiation incident (1000 W/m^2).

The current-voltage (I-V) relationship of a solar cell equivalent circuit is given by,

$$I = I_{ph} - I_s\left\{\left[\frac{q\left(V + IR_s\right)}{AKT_c}\right] - 1\right\} - \frac{V + IR_s}{R_{sh}} \quad (9)$$

where I_{ph}, I_s, q, R_s, A, K, T_c, R_{sh}, V, and I are photogenerated current, reverse saturation current, electron charge, series resistance, ideality factor, Boltzmann constant, cell temperature, shunt resistance, voltage, and current.

The power output (P) from a solar cell is estimated by,

$$P = V * I = FF * \left(I_{sc} * V_{oc}\right) \quad (10)$$

where FF, I_{sc}, V_{oc} are fill factor, short circuit current, and open-circuit voltage.

3.2 Exergy efficiency

The exergy of a PV system is calculated by taking into account the amount of energy that is lost owing to the creation of entropy in a system [36]. The exergy of a substance is expressed in terms of its ability to produce work that is beneficial to the environment. Exergy analysis is used to determine PV system losses and energy availability. System improvement is being studied in terms of thermodynamic analysis[37]. The exergy is given as follows[38],

$$E_x = H - H_0 - T_0\left(S - S_0\right) \quad (11)$$

The exergy of solar radiation [39-41],

$$E_{x,in} = \left(a - \left[\frac{T_a}{T_s}\right]\right) I_s A \quad (12)$$

The exergy of solar PV system [39-41],

$$E_{x,pv} = E_{x,elec} + E_{x,therm} + E_{x,distortion}$$
$$E_{x,pv} = V_m I_m - \left(1 - \frac{T_a}{T_{cell}}\right) h_{ca} A\left(T_{cell} - T_a\right) \quad (13)$$

$$Exergy\ efficiency = \frac{Output\ exergy}{Input\ exergy} \quad (14)$$

$$= \frac{V_m I_m - \left(1 - \frac{T_a}{T_{cell}} h_{ca}\left(T_{cell} - T_c\right)\right)}{\left(1 - \frac{T_a}{T_s}\right) I_s A} \quad (15)$$

4. RESULTS AND DISCUSSION

Figure 3 shows the variations in total solar radiation variation at Chennai, Bengaluru, Thiruvananthapuram, and Hyderabad on different PV module tilt angles. There was a maximum level of reflected solar radiation at the four distinct sites, as shown on the graph. Solar panels can be tilted up to 30^0 in any direction. Each station was able to get the best possible angle for maximum solar radiation, based on its location. The best tilt angles for Chennai, Bengaluru, Thiruvananthapuram, and Hyderabad were 25^0, 30^0, 20^0, and 30^0 while the total solar radiations at this angle were 704 W/m^2, 722 W/m^2, 693 W/m^2, and 774 W/m^2 correspondingly. Surface reflectivity of 0.07 reduced the optimal tilt angle for Chennai, Bengaluru, Thiruvananthapuram, and Hyderabad to 15^0, 20^0, 10^0, and 20^0 correspondingly, and the total solar radiations at this angle were 698 W/m^2, 702 W/m^2, 685 W/m^{2}and 702 W/m^2 respectively.

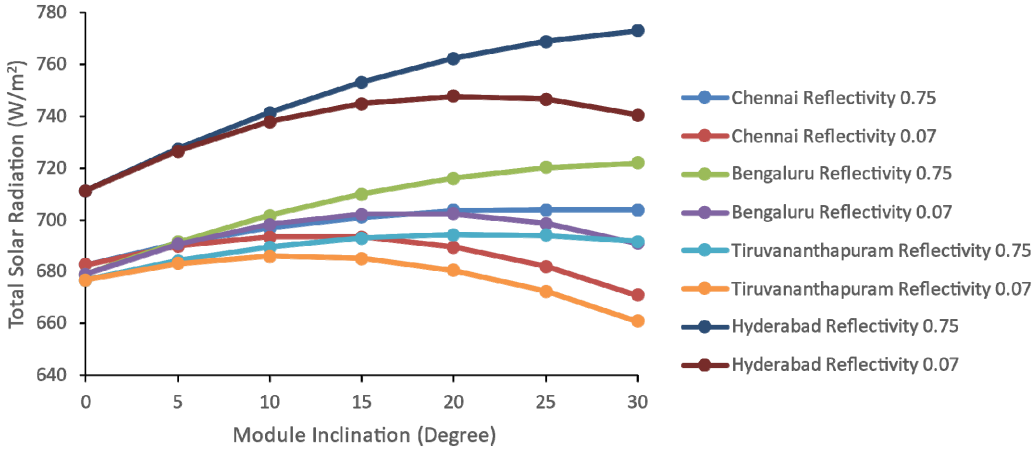

Figure 3. Total solar radiation variation with module inclination for Chennai, Bengaluru, Thiruvananthapuram, and Hyderabad

The total solar radiation levels for four separate locations at the optimal tilt angle of their corresponding surface reflectivity value were 0.85%, 2.77%, 1.15%, and 9.31% accordingly. Figure 4 shows the current variations at Chennai, Bengaluru, Thiruvananthapuram, and Hyderabad with the same isotropic and reflectivity (0.07) for 0^0 PV module inclination angle. Similarly, current variations at the above-mentioned locations were studied with the same isotropic and reflectivity (0.07) at 5^0, 10^0, 15^0, 20^0, 25^0, and 30^0.

Except for the Thiruvananthapuram location, the output voltage was essentially constant at whatever inclination angle. As the inclination angle increased, the current flow decreased generally. Later on, the current increased for 10^0 and 15^0 of inclination angle. Finally, an increase in inclination angle decreased the PV module output current. According to this, it was obvious that the ideal tilt angle of inclination for solar panels in the southern Indian region was between 10^0 and 15^0, irrespective of location. It was shown that the change in current and voltage deviation levels dropped by 5.62%, 10.83%, 2.11%, and 16.07%accordingly at 0^0 to 30^0 tilt angles (Chennai, Bengaluru, Thiruvananthapuram, and Hyderabad).

Figure 5 shows the current variations at Chennai, Bengaluru, Thiruvananthapuram, and Hyderabad on the same isotropic and reflectivity (0.75) for 0^0 PV module inclination angle. Maximum output current obtained and deviations of voltage are minimum for all the installed PV locations for the tilt angles of 0^0 and 5^0 inclinations. This can be varied for inclination increases up to 20^0 inclinations of PV module and current leading to major deviations compared with the lower tilt angle of PV modules. A gradual decrease in the output current was observed at $25^0$and 30^0inclinations. There was a 14.03%, 5.35%, and 11.32% drop in the current and voltage deviation levels at $0^0$to 30^0tilt angles, respectively.

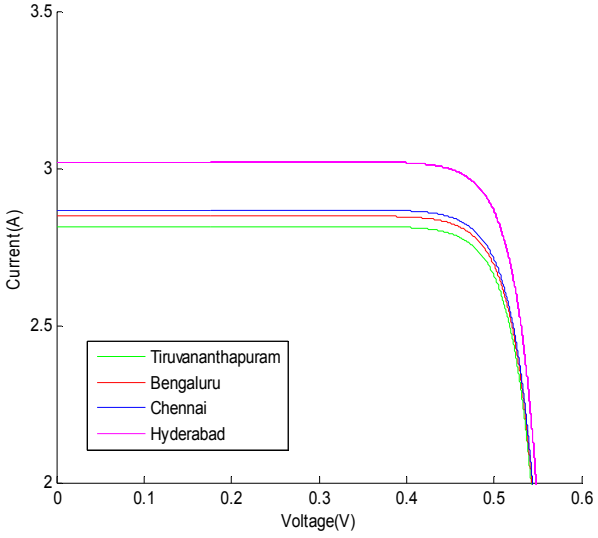

Figure 4. Current variation with voltage under same Isotropic and reflectivity (0.07) in different locations for module inclination angle of 0^o

Figures 6(a)-6(d) show the percentage change in output parameters (current and voltage) with tilt angle for increases in ground albedo from 0.07 to 0.75 at Hyderabad, Chennai, Bengaluru, and Thiruvananthapuram. Figure 6(a) shows the highest percentage changes in the value of both current and voltage that can be obtained at a tilt angle of 10^0 are 6.77 A and 3.571 V respectively with a ground albedo of 0.75. Changes in voltage achieved are better than the current value for increases with ground albedo from 0.07 to 0.75 at Hyderabad. Figure 6(b) shows the maximum change in current and voltage (negative side) at a tilt angle of 10^0 for ground albedo value as 0.07 considered more suitable compared with the highest ground albedo value. Figures 6(c) and 6(d) provide the mixed responses to both changes in current and voltage at tilt angles between 5^0 to 15^0. It shows a change in current as a maximum at a ground albedo of 0.07 (negative side) than 0.75. Figure 6(d) shows a change in voltage as almost zero for four tilt angle (0^0, 15^0, 25^0, and 30^0) positions and changes in currently available is maximum at a tilt angle of 5^0 and 10^0.

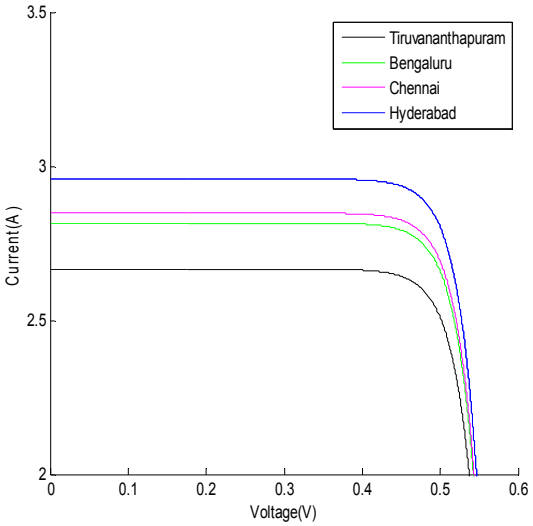

Figure 5. Current variation with voltage under same Isotropic and reflectivity (0.75) in different locations for module inclination angle of 0^0

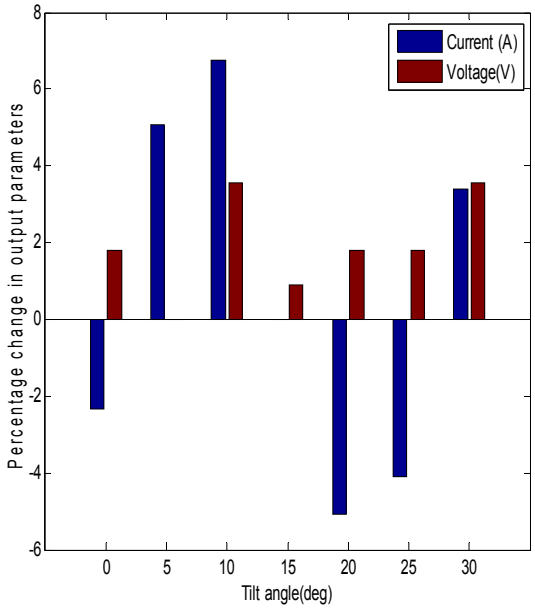

Figure 6(a). Percentage change in output parameters (Current and Voltage) with tilt angle for increases in ground albedo from 0.07 to 0.75 at Hyderabad

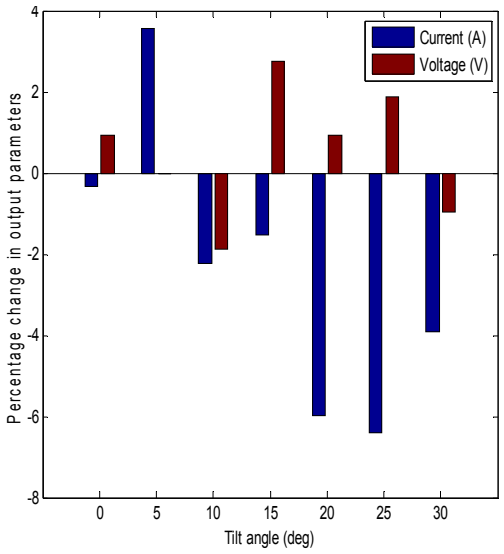

Figure 6(b). Percentage change in output parameters (Current and Voltage) with tilt angle for increases in ground albedo from 0.07 to 0.75 at Chennai

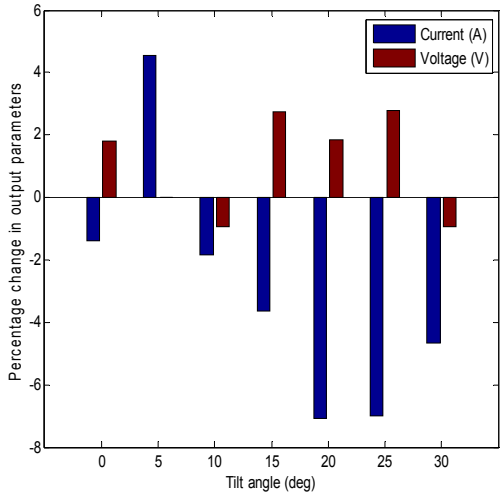

Figure 6(c). Percentage change in output parameters (Current and Voltage) with tilt angle for increases in ground albedo from 0.07 to 0.75 at Bengaluru

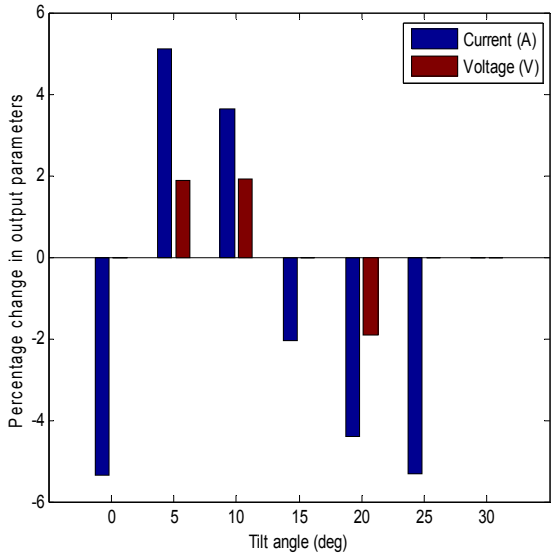

Figure 6(d). Percentage change in output parameters(Current and Voltage) with tilt angle for increases in ground albedo from 0.07 to 0.75 at Thiruvananthapuram

Total solar radiation variations for December 2014, January, and February 2015 are depicted in Figure 7 with an inclination angle of 13^0 degrees, the solar panel array was pointing south. It was situated on a 0.22 reflectivity concrete rooftop. The solar meter recorded the amount of solar radiation that fell on the PV surface in December 2014, January, and February 2015. It was measured from 9 am to 4 pm on an experimental day as shown in Figure7. The monthly variations of exergy efficiencies and solar radiation variation of a solar PV module are shown in Figure 8. In the analysis of solar radiation, availability is obtained maximum and minimum of 1178 and 751 W/m^2 on during April and November respectively. Exergy efficiency, as a function of solar radiation level on the surface of solar PV module and it is a maximum of 21.38%, when the lower solar radiation availability during the November month and minimum of 13.63%, when the maximum solar radiation availability of April month in a year respectively.

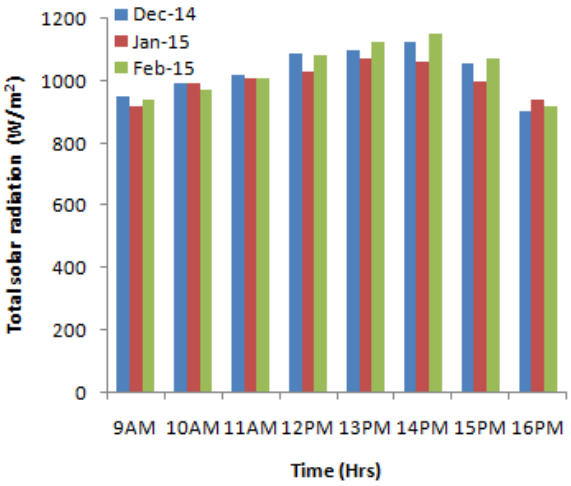

Figure 7. Average total solar radiation variation with time for three months

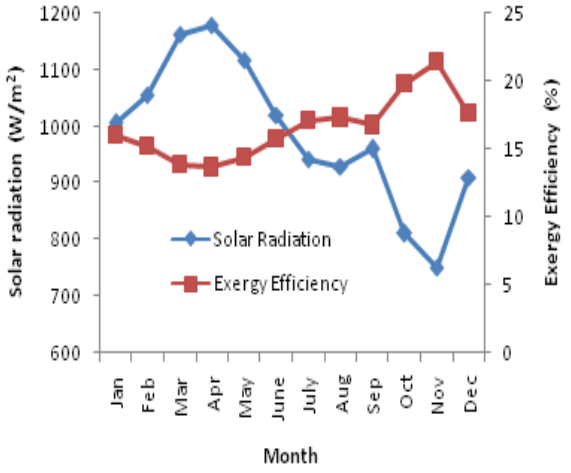

Figure 8. Monthly variations of exergy efficiency and solar radiation variation of a solar PV module

The effect of temperature on solar PV module exergy efficiency is shown in Figure 9. The average exergy efficiency varied between initial and final values by approximately 36.42% with the corresponding increase in solar PV module temperature of 10.51%. The exergy efficiency is a maximum of 18.23% isobserved ata PV module temperature of 298 K.

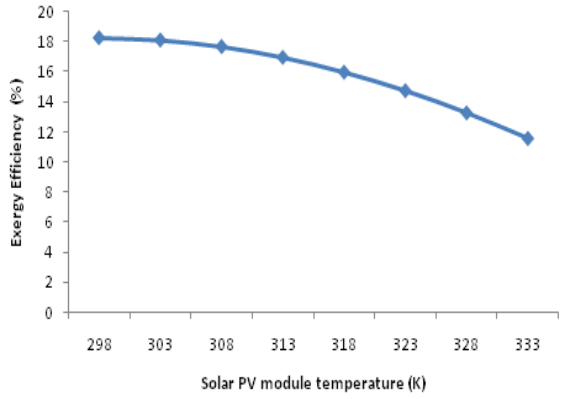

Figure 9. Variations in exergy efficiencies of solar PV module temperature

5. CONCLUSION

The results of this study indicate that the surface ground reflectivity plays a vital role depending on the amount of solar radiation falling on PV modules. The solar radiation received by the PV module had a ground reflectance ranging from 0.7 to 0.75 depending on the location. Tilt angle from 10^0 to 20^0 with a ground albedo of 0.07 has shown the maximum output current for southern India with no change at the voltage level. The tilt angle ideal for Chennai, Bengaluru, Thiruvananthapuram, and Hyderabad were 15^0 and 25^0, 20^0 and 30^0, 10^0 and 20^0, and 20^0 and 30^0 under albedo of 0.07 and 0.75 correspondingly for the four cities. At albedos of 0.07 and 0.75, the change in current and voltage was at its peak. Ground albedo was altered from 0.07 to 0.75, and the corresponding % variations in voltage and current were 3.571V and 6.77 A at a tilt angle of 10^0 in South India. The maximum exergy efficiency is 18.23%, while the temperature of the solar PV module is 298 K. The maximum and minimum values of exergy efficiency are 21.38% and 13.63%, respectively.

REFERENCES

[1] Burg, Brian R., Patrick Ruch, Stephan Paredes, and Bruno Michel. "Effects of radiative forcing of building integrated photovoltaic systems in different urban climates." Solar Energy, vol: 147, 2017, pp: 399-405.

[2] Wang, Lunche, Ozgur Kisi, Mohammad Zounemat-Kermani, Germán Ariel Salazar, Zhongmin Zhu, and Wei Gong. "Solar radiation prediction using different techniques: model evaluation and comparison." Renewable and Sustainable Energy Reviews 61 (2016): 384-397.

[3] Shukla, K.N., Saroj Rangnekar, Sudhakar, K., "Comparative study of isotropic and anisotropic sky models to estimate solar radiation incident on the tilted surface: A case study for Bhopal, India: Energy Reports, Vol: 1, (2015), pp:96-103.

[4] Kotak, Y., Gul, M.S., Muneer, T., Ivanova, S.M., "Investigating the impact of ground albedo on the performance of PV systems", In proceedings of CIBSE Technical Symposium, London, UK, 2015, pp: 16-17.

[5] Kumar, A., Gomathinayagam, S., Giridhar, G., Mitra, I., Vashista, R., Meyer, R., Schwandt, M., Chhatbar, K., "Field experience with the operation of solar radiation resource assessment stations in India, Energy Procedia, Vol:49, (2014), pp: 2351-2361.

[6] Meyta, R.V., Savrasov, F.V.: "To study the influence of snow cover on the power generated by photovoltaic modules", In IOP Conference Series: Materials Science and Engineering, Vol: 81, No:1, pp: 1-5, 2015, IOP publishing.

[7] IoanSarbu, Calin Sebarchievici, Chapter 2 - Solar Radiation, Solar Heating and Cooling Systems, Academic Press, 2017, Pages 13-28, ISBN 9780128116623.

[8] Samy A. Khalil, Shaffie, A.M., "Performance of statistical comparison models of solar energy on horizontal and inclined surface", International Journal of Energy and Power, Vol:2, Issue :1, 2013(a), pp:8-25.

[9] Samy A.Khalil, Shaffie, A.M., "A comparative study of total, direct and diffuse solar irradiance by using different models on horizontal and inclined surfaces for Cairo, Egypt", Renewable and Sustainable Energy Reviews, Vol: 27, pp:853-863, 2013(b).

[10] Peled, A., Appelbaum, J., "Minimizing the current mismatch resulting from different locations of solar cells within a PV module by proposing new interconnections", Solar Energy, Vol:135, 2016, pp:840-867.

[11] Shunlin Liang, Xiaowen Li, Jindi Wang, Chapter 7 - Broadband Albedo, Advanced Remote Sensing, Academic Press, 2012, Pages 175-233, ISBN 9780123859549.

[12] Khatib, T., Mohamed, A., Mahmoud, M., Sopian, K., "Optimization of the tilt angle of solar panels for Malaysia", Energy Resources, part A: Recovery, Utilization, and Environmental Effects, Vol: 37, No: 6, 2015, pp: 606-613.

[13] Emanuele Calabro, "An algorithm to determine the optimum tilt angle of a solar panel from global horizontal solar radiation", Journal of Renewable Energy, Vol: 2013, pp:12 pages.

[14] Seung-Ho yoo, "Simulation for an optimal application of BIPV through parameter variation", Solar Energy, Vol:85, 2011, pp:1291-1301.

[15] Appelbaum, J., "Current mismatch in PV panels resulting from different locations of cells in the panel", Solar Energy, Vol: 126, 2016, pp:264-275.

[16] Bezari, S., Bekkouche, S. M., &Benchatti, A. (2021) Investigation and improvement for a solar greenhouse using sensible heat storage material. FME Transactions, 49(1), 154-162.

[17] Rehman S., Aliyu K.N., Alhems L.M., Mohandes M.A., Himri Y., Allouhi A., (2021). A Comprehensive Global Review of Building Integrated Photovoltaic Systems, FME Transactions, March 2021, 49(2), 253-268).

[18] Rehman, S., &Mohandes, M. (2008). Artificial neural network estimation of global solar radiation using air temperature and relative humidity. Energy Policy, 36(2), 571-576).

[19] Rehman, S., & Halawani, T. O. (1997). Global solar radiation estimation. Renewable Energy, 12(4), 369-385.

[20] Rehman, S., &Mohandes, M. (2012). Splitting global solar radiation into diffuse and direct normal fractions using artificial neural networks. Energy Sources, Part A: Recovery, Utilization, and Environmental Effects, 34(14), 1326-1336.

[21] Mohandas, M., Rehman, S., & Halawani, T. O. (1998). Estimation of global solar radiation using artificial neural networks. Renewable energy, 14(1-4), 179-184.

[22] Rehman, S. (1998). Solar radiation over Saudi Arabia and comparisons with empirical models. Energy, 23(12), 1077-1082.

[23] Mohandes, M., & Rehman, S. (2010). Global solar radiation maps of Saudi Arabia. Journal of Energy and Power Engineering, 4(12), 57-63.

[24] Rehman, S., &Mohandes, M. (2009). Estimation of a diffuse fraction of global solar radiation using artificial neural networks. Energy Sources, Part A, 31(11), 974-984.

[25] Rehman, Shafiqur, & Ghori, Saleem G. Spatial estimation of global solar radiation using geostatistics. The United Kingdom.

[26] Aksakal, A., & Rehman, S. (1999). Global solar radiation in northeastern Saudi Arabia. Renewable Energy, 17(4), 461-472.

[27] Hussain F.M., Rehman S., Al-Sulaiman F.A., (2020). Performance Evaluation of a Solar Chimney Power Plant for Varied Climatic Conditions, FME Transactions 49(1), 64-71.

[28] Rehman, S., &Sahin, A. Z. (2016). A wind-solar PV hybrid power system with battery backup for water pumping in remote localities. International Journal of Green Energy, 13(11), 1075-1083.

[29] Margaritou, M. D., &Tzannatos, E. (2018). A multi-criteria optimization approach for solar energy and wind power technologies in shipping. FME Transactions, 46(3), 374-380.

[30] Mohandes, M. K. S. R. M., Balghonaim, A., Kassas, M., Rehman, S., & Halawani, T. O. (2000). Use of radial basis functions for estimating monthly mean daily solar radiation. Solar Energy, 68(2), 161-168.

[31] Solar radiation of South India and entire India representation map retrieved from http:// www.mapsofindia.com, 09th September 2016.

[32] Khasawneh, Q.A., Damra, Q.A., Salman, O.H.B., "Determining the optimum tilt angle for solar applications in Northern Jordan", Jordan Journal of Mechanical and Industrial Engineering, Vol: 9, No:3, 2015, pp: 187-193.

[33] Sekar, M., Sakthivel, M., Satheesh Kumar, S., Ramesh, C., "Estimation of global solar radiation for Chennai", European Journal of Scientific Research, Vol:73, No:3, pp:415-424, 2012.

[34] Ajit P.Tyagi, "Solar radiant energy over India", India meteorological department, Ministry of earth sciences, 2009.

[35] Kumar, R.A., Babu, B.G. and Mohanraj, M., 2016. Thermodynamic performance of forced convection solar air heaters using pin-fin absorber plate packed with latent heat storage materials. Journal of Thermal Analysis and Calorimetry, 126(3), pp.1657-1678.

[36] Pandey, A.K., Tyagi, V.V., Rahim, N.A., Kaushik, S.C. and Tyagi, S.K., 2015. Thermal performance evaluation of direct flow solar water heating system using exergetic approach. Journal of Thermal Analysis and Calorimetry, 121(3), pp.1365-1373.

[37] Petela, R., 2003. Exergy of undiluted thermal radiation. *Solar Energy*, *74*(6), pp.469-488.

[38] Joshi, A.S., Dincer, I. and Reddy, B.V., 2009. Thermodynamic assessment of photovoltaic systems. *Solar Energy*, *83*(8), pp.1139-1149.

[39] Taguchi, M., Terakawa, A., Maruyama, E. and Tanaka, M., 2005. Obtaining a higher Voc in HIT cells. *Progress in photovoltaics: research and applications*, *13*(6), pp.481-488.

[40] Markvart, T., 2003, Solar electricity, second edition, John wiley& sons Ltd., Chichester, UK.

[41] Benghanem, M., "Optimization of tilt angle for solar panel: A case study for Madinah, Saudi Arabia", Applied Energy, Vol:88, 2011, pp:1427-1433.

NOMENCLATURE

ϕ	Latitude
Δ	declination angle
ω_{ss}	Sunset hour angle for the mean day of the month
ω'_{ss}	Sunset hour angle for the tilted surface for the mean day of the month
H_g	Monthly mean daily global radiation on a horizontal surface
R_b	The Ratio of average daily beam radiation on a tilted surface and average daily beam radiation on the horizontal surface
H_d	Monthly mean daily diffuse radiation on a horizontal surface
β	The tilt angle of the solar panel
ρ	Ground albedo
R_d	The Ratio of the average daily diffuse radiation on a tilted surface and average daily diffuse radiation on a horizontal surface
Ex	Exergy of substance
H	Enthalpy of substance
Ho	Enthalpy at environment condition of substance
S	Entropy of substance
So	Entropy at environment condition of substance
T_a	Ambient temperature (K)
T_s	The temperature of the sun which is taken

	as 5777K
I_s	Solar radiation (W/m^2)
A	Area of the solar PV module (m^2)
$E_{x,elec}$	The exergy efficiency of an electrical system
$E_{x,\ therm}$	The exergy efficiency of the thermal system
$E_{x,distortion}$	Exergy efficiency on Internal and external heat loss
$E_{x,\ PV}$	Exergy of solar PV system

ТЕРМОДИНАМИЧКА АНАЛИЗА РЕФЛЕКТОВАНОГ СОЛАРНОГ ЗРАЧЕЊА НА НАГНУТИМ ПВ МОДУЛИМА У ЈУЖНОЈ ИНДИЈИ

А.А. Дас, Д.Р. Пател

Неопходан је значајан обим енергије за задово–љавање растуће потражње за енергијом као резултат брзог раста становништва и промена начина живота у друштву. Нагнути ПВ модул побољшава рад и смањује ризике везане за производњу, пренос и коришћење електричне и топлотне енергије без икаквих деградација у климатским условима (попут конвенционалних извора енергије). И фиксни и нагнути системи ПВ модула примају високо долазно сунчево зрачење. У овој студији је извршена анализа излазне струје и напона за различите углове нагиба од 0º до 30º за различите јужне делове Индије (Ченеј, Бенгалуру, Тируванантхапурам и Хајдерабад). Одра–жени албедо фактор се узима у обзир за различите локације у распону од 0,07 до 0,75 са параметрима струјног напона. Уочене су варијације углова нагиба фотонапонских модула са варија–цијама у укупном сунчевом зрачењу под различитим вредностима ал–беда тла. Проучаване су промене струје и напона са углом нагиба на различитим локацијама. Анализи–ране су месечне варијације и ефекти температуре на ексергијска ефикасност и сунчево зрачење.